Adiabatic Normal Zone Development in MgB_2 Superconductors

H. van Weeren, N. C. van den Eijnden, W. A. J. Wessel, P. Lezza, S. I. Schlachter, W. Goldacker, M. Dhallé, A. den Ouden, B. ten Haken, and H. H. J. ten Kate

***Abstract*—A-priori knowledge of the normal zone development in MgB_2 conductors is essential for quench protection of applications. Therefore the normal zone propagation in a monofilament MgB_2/Fe conductor under near-adiabatic conditions at 4.2 K has been measured and simulated. The results show normal zone propagation velocities up to several meters per second. In addition, by including the voltage-current relation into the computational model, the influence of the n-value on the normal zone propagation is determined. The simulations show that lower n-values suppress the normal zone propagation velocity due to lower heat generation in the MgB_2 filaments.**

***Index Terms*—MgB_2 superconductors, normal zone propagation.**

I. Introduction

UNDERSTANDING of the normal zone behavior in MgB_2 composite superconductors is essential for the quench protection of applications that are based on this material. From this point of view it is desirable that a composite conductor exhibits a sufficiently large normal zone propagation velocity (V_{NZ}). A fast normal zone development creates a large area where stored energy is dissipated, limiting the hot spot temperature, and it makes it easier to detect the existence of a normal zone. The development of the normal zone depends on the operating current, on the steepness of the voltage-current characteristic, on current-and heat diffusion and finally on the temperature margin [1], [2].

Previously the influence of the diffusivity on the normal zone development in MgB_2 conductors was studied by means of simulations with copper and iron sheathed conductors. The propagation velocities that were calculated agree with first measurements by Fu *et al.* [3]. Here V_{NZ} measurements and simulations on a mono-filament MgB_2/Fe conductor are presented. The measurements and simulations are compared to validate the computational model for MgB_2 conductors. The measurements are performed under quasi adiabatic conditions. In this way, the lateral cooling via boiling helium is excluded, so that information on the intrinsic normal zone development of MgB_2 conductors is obtained. Moreover, a quasi adiabatic set-up is suitable for experiments at the anticipated operating temperatures, ranging between 15 and 30 K.

Secondly, the influence of the n-value on the V_{NZ} is simulated. The n-value becomes important when electrical conductivity of the matrix becomes comparable to the electrical conductivity of MgB_2. In this case the heat generation in the filaments cannot be neglected anymore.

Manuscript received October 3, 2004. This work was supported by the Dutch Technology Foundation STW.

H. van Weeren, N. C. van den Eijnden, W. A. J. Wessel, M. Dhallé, A. den Ouden, B. ten Haken, and H. H. J. ten Kate are with the University of Twente, NL 7500 AE Enschede, The Netherlands (e-mail: h.vanweeren@tnw.utwente.nl).

P. Lezza is with the University of Geneva, CH 1211 Geneva-4.

S. I. Schlachter and W. Goldacker are with the Forschungszentrum Karlsruhe, GE 76021 Karlsruhe, Germany.

Digital Object Identifier 10.1109/TASC.2005.849227

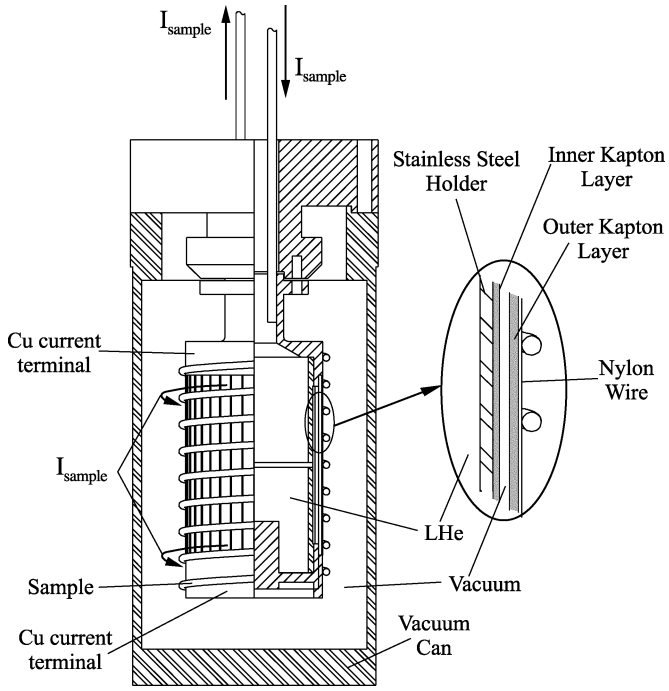

Fig. 1. Schematic view of the quasi adiabatic NZP insert. The right half of the drawing shows the cross-section of the sample holder wall.

II. Normal Zone Propagation

A. Experimental Set-Up

Measurements of the V_{NZ} are performed with the insert as depicted in Fig. 1. The insert is emerged in a LHe bath inside the bore of a 15 T magnet. The sample is reacted in a helical shape and mounted tightly on the sample holder. The ends of the sample are soldered to the copper current terminals. To provide enough, cooling for the normal conducting current terminals, the inside of the sample holder has an open connection to the LHe bath.

The quasiadiabatic condition is attained by evacuating the vacuum can, leaving only a small amount of radiative heat flux from the sample to the vacuum can. To minimize the heat flow

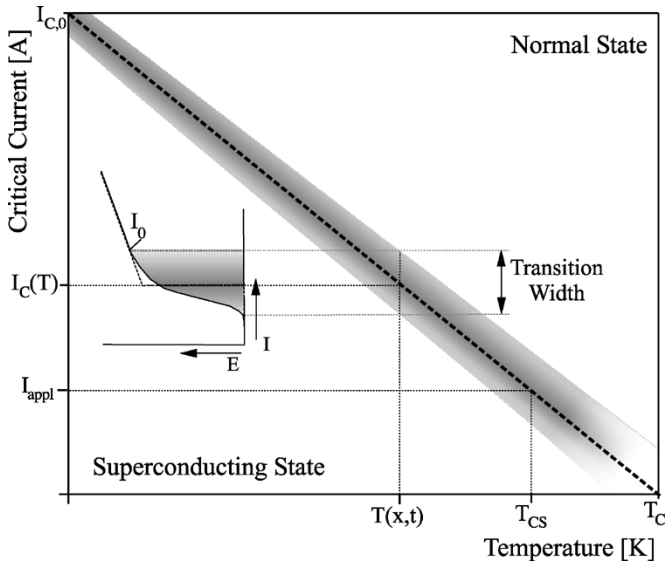

Fig. 2. $I_c(T)$ curve of MgB_2 (dotted line). The shaded area around the $I_c(T)$ line represents the transition width (i.e. it is the voltage-current transition projected on the $I_c(T)$ line (inset)).

from the sample to the LHe inside the sample holder, the sample holder consists of an inner and outer Kapton layer with vacuum in-between. The sample holder and the sample are further thermally detached with nylon wires that are placed between the sample and the outer Kapton layer. In this way only small point contacts between the nylon wires and the sample exist.

The normal zone propagation is measured with the voltage-time-of-flight method. To initiate the propagating normal zone, a heat pulse is applied to the sample with a wire-wound heater.

B. Numerical Modeling

The numerical code is based on an explicit finite difference scheme that solves the well-known one-dimensional heat balance equation. The numerical scheme accounts for all relevant temperature-and field dependent material properties (i.e. ρ, κ, C, J_c and n-value). With this model the classical concept of current sharing is refined [1]. This refinement is based on a parallel path approach between the superconductor and the matrix that accounts also for the heat generated in the filaments. Fig. 2 depicts the critical current vs. temperature line (bold, dashed line). If the temperature rises due to a thermal disturbance, I_c decreases following the $I_c(T)$ line. In the classical current sharing concept, I_c drops below the transport current I_{appl} when the temperature passes T_{cs} and the current will then be shared between the filaments and the matrix. The filaments continue to carry $I_c(T)$, while the excess current $I_{appl} - I_c(T)$ is carried by the matrix. Only the excess current in the matrix is assumed to cause ohmic heating.

This classical current sharing concept is only valid when 1) a sharp voltage-current transition of the superconducting filaments is considered; and 2) when the electrical resistivity of the matrix is much lower than the normal state resistivity of the filaments. This is indeed the case for Nb_3Sn and NbTi conductors that usually have high n-values and a low resistive copper matrix. Accordingly, the classical current sharing concept works very well for these materials.

However, when a lower n-value is considered, which is the case for HTS and some MgB_2 conductors, the voltage-current transition of the filaments has to be included. We assume that the voltage-current relation of the superconducting filaments can be described by a power law

$$E = E_c \left(\frac{J_{sc}}{J_c}\right)^n \tag{1}$$

and define the electrical field E_0 and current density $J_0 (= I_0/A_{sc})$ as the point where dissipation in the superconducting and normal conducting state become equal

$$E_0 = E_c \left(\frac{J_0}{J_c}\right)^n = \rho_{sc} J_0 \tag{2}$$

Considering the same temperature increase as before, the voltage in the filaments is already rising well before $I_0(T)$ meets the transport current (see Fig. 2). Current is already shared and heat is accordingly generated. After $I_0(T)$ has passed the transport current the transition is complete and the filaments continue to obey ohm's law. By considering the smooth voltage-current transition with a finite resistance after the transition, heat generation in the filaments around the normal zone front is not neglected anymore. This heat generation depends on the steepness of the voltage-current transition. The following heating function can then be derived:

$$I_{appl} = \begin{cases} A_m \frac{E}{\rho_m} + A_{sc}\left(J_c\left(\frac{E}{E_c}\right)^{\frac{1}{n}}\right) & E < E_0 \\ A_m \frac{E}{\rho_m} + A_{sc}\frac{E}{\rho_{sc}} & E > E_0 \end{cases} \tag{3}$$

$$G = E \cdot I_{appl} \tag{4}$$

Here E_c is the voltage criterium; J_c is the critical current; J_{sc} is the current density in the filaments; ρ_m and ρ_{sc} are the electrical resistivities of the matrix and the filaments in the normal state; A_m and A_{sc} are respectively the cross-sectional areas of the matrix and the superconducting filaments.

The full $J_c(B,T)$ and $n(B,T)$ surfaces of a given MgB_2 sample are usually not available. In the absence of generally accepted scaling relations such as those for Nb_3Sn [4], we use the $J_c(B,T)$ and $n(B,T)$ formulations that were established for MgB_2 bulk [5]. Also, since the heat generation in the filaments plays an important role when a poor conducting matrix is considered, the MgB_2 data on thermal- and electrical conductivity, as well as heat capacity as function of field and temperature become very important. Again, we used data obtained on bulk by Wang *et al.* and Schneider *et al.* [6], [7].

III. Results and Discussion

A. Measurements Versus Calculations

Both measurements and simulations on the normal zone propagation have been performed on a mono-filament MgB_2/Fe tape at 4.2 K. Fig. 3 depicts the normal zone propagation velocity versus the transport current at 4 and 5 T. For comparison, measurements and calculations on a PIT Nb_3Sn conductor are included [8], [9].

As far as quench protection is concerned a high V_{NZ} is desirable. Fig. 3 shows that the MgB_2 conductor exhibits lower

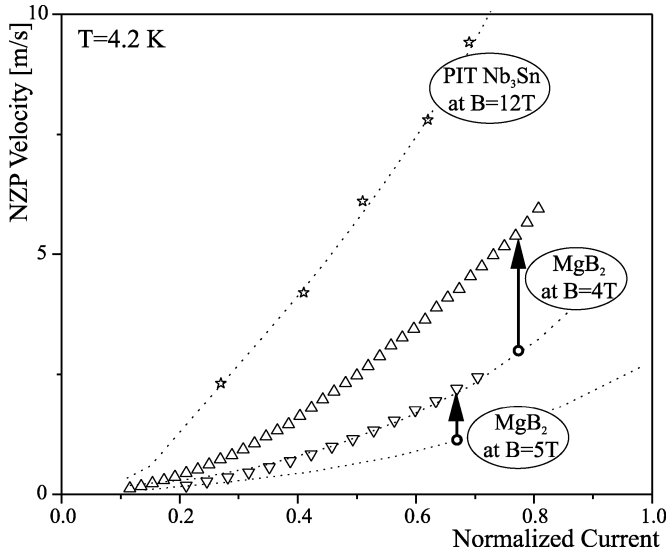

Fig. 3. NZP velocity measurements of MgB_2/Fe mono-filament conductor as function of normalized current at $B = 4$ ($I_c = 260$ A) and 5 T ($I_c = 142$ A). Its dimensions are 4 by 0.4 mm^2 with a filling factor of approximately 31%. The dotted lines are the corresponding numerical simulations. As comparison measurements and calculations of a PIT Nb_3Sn/Cu conductor at 12 T ($I_c = 291$ A) are included (diameter is 0.9 mm. with a filling factor of 45%).

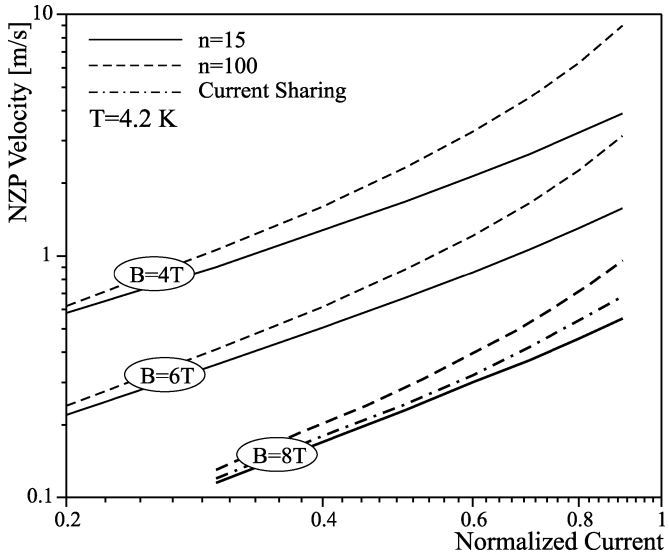

Fig. 4. Simulations of an MgB_2/Fe conductor with an n-value of 15 compared to a hypothetical similar conductor with an n-value of 100. As comparison, calculations at $B = 8$ T based on the current sharing concept are included (dash-dotted line). The critical current are 555 A, 155 A and 39 A at 4, 6 and 8 T respectively. Its diameter is 1.1 mm with a filling factor of 42%.

propagation velocities than the Nb_3Sn conductor. This is partly caused by the lower transport current that is carried by MgB_2 conductors, resulting in a lower heat generation. More important is the fact that the iron matrix of the MgB_2 conductor is a rather poor conductor in comparison with the copper matrix of the Nb_3Sn conductor, reducing the heat diffusion significantly. Nevertheless, the MgB_2 conductor shows "real" propagation of a normal zone as opposed to HTS conductors that exhibit a quasi static heating of the normal zone.

The calculations of the V_{NZ} of the Nb_3Sn and the corresponding measurements show an excellent agreement. In contrast, the measurements of the MgB_2 conductor are a factor of 2 higher than predicted by the calculations. The main reason for this discrepancy is its large single filament. The dimension of this filament is about 200 μm in height and about 3 mm in width. In contrast, the Nb_3Sn has 504 filaments with a diameter of approximately 20 μm. This means that the lateral diffusion of current from the filaments to the matrix is more efficient in the Nb_3Sn conductor than in the MgB_2 conductor. Because of this slow current diffusion, heat generation in the MgB_2 filament is larger than accounted for in the 1-dimensional model (that implicitly assumes an infinitely fast lateral diffusion). However, as MgB_2 conductor development proceeds, the filament size will decrease and the 1-dimensional assumption will become more realistic. Our results show that V_{NZ} can be expected to decrease accordingly.

B. Influence of the Exponential n-Value

In order to demonstrate the effect of the n-value on the normal zone propagation, we used $J_c(B,T)$ and $n(B,T)$ data measured on a conductor by Goldacker *et al.* [10]. Although these conductors have a very good $I_c(B)$ performance, they have a rather low n-value of about 15. This implies that the heating function around the normal zone front will be very smooth. The influence of this low n-value is studied numerically by comparing the results with a similar hypothetical conductor that has an n-value of 100. The results of the normal zone propagation velocities are depicted in Fig. 4.

It can be seen that for all applied magnetic fields, the hypothetical conductor has a higher propagation velocity than the actual conductor with an n-value of 15. Furthermore, the hypothetical conductor shows an upturn with increasing transport current. The differences in V_{NZ} behavior between the two conductors reflect the effect of the heat generation in the filaments when the voltage-current relation is included in the model.

The significance of the voltage-current relation is explained by Fig. 5, where the heat generation as function of temperature is plotted. The heat generation in the filaments, which is neglected in the current sharing concept, causes the difference in V_{NZ} for the two different n-values (see Fig. 4). This heating is reflected in the form of a bump in-between the classical T_{CS} and T_C. At T_{CS} the voltage starts to rise, causing heating in the filaments and current slowly starts to diffuse in the matrix. The top of the bump is the moment where the effective resistance of the filaments equals the resistance of the matrix. After this point the effective resistance becomes higher than the resistance of the matrix, decreasing the current and the heat generation in the filaments. The point where heating in the filaments becomes significant is related to the steepness of the voltage-current relation. After the transition ($T > T_C$) the heat generation does not return to zero. This is the consequence of the parallel path assumption and the fact that the resistances of MgB_2 and Fe are in this case quite comparable.

As pointed out earlier, the $V_{NZ}(I/I_c)$ characteristic for $n = 100$ shows an upturn relative to the characteristic for $n = 15$. This is caused by the phenomena that with increasing current the cumulative heat generation in the filaments around the normal zone front (the bump) grows faster for higher n-values.

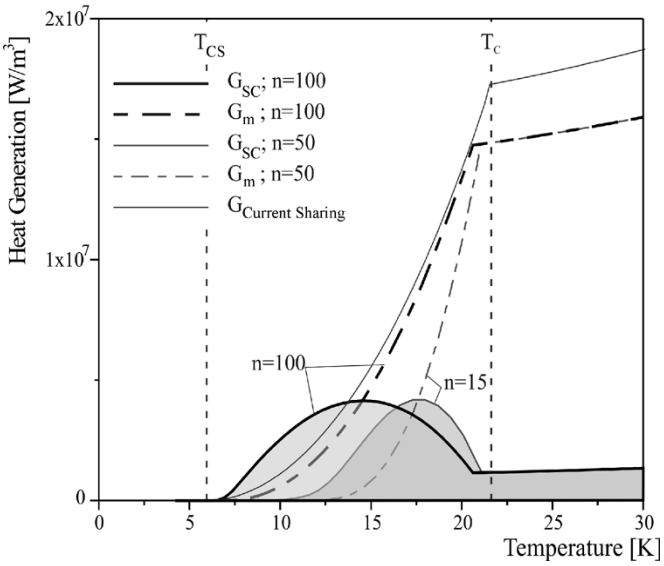

Fig. 5. Heat generation around the normal zone front between the classical T_{CS} and T_C at 8 T and a normalized current of 0.9 for $\mathrm{n} = 100, \mathrm{n} = 15$ and according to the current sharing concept. The monotonously increasing curves indicate the heat generation in the matrix, while the peaked curves indicate the heat generation in the filaments.

IV. Conclusions

To study the normal zone development in composite conductors a 1-dimensional computational model was developed. To account for smooth voltage-current transition and heat generation in the filaments, the model is provided with a heating function that is based on a parallel path between the superconducting filaments and the matrix.

To validate the model we have performed adiabatic normal zone propagation experiments with both $\mathrm{Nb_3Sn}$ and $\mathrm{MgB_2}$ conductors. Good agreement exists between the simulations and the measurements of the $\mathrm{Nb_3Sn/Cu}$ conductor with fine filaments. In contrast, our 1-dimensional model does not describe the experiments with the mono-filament $\mathrm{MgB_2/Fe}$ conductor accurately. This is caused by the slow lateral current diffusion in mono-filament conductors and the lack of properly described material properties of a given $\mathrm{MgB_2}$ sample.

Simulations have been performed to study the influence of the n-value on the normal zone propagation. The calculations show that a lower n-value suppresses the normal zone propagation velocity due to lower heat generation around the normal zone.

References

[1] M. N. Wilson, *Superconducting Magnets*: Oxford Science Publications, 1986.

[2] A. L. Rakhmanov, V. S. Vysotsky, Y. A. Ilyin, T. Kiss, and M. Takeo, "Universal scaling law for quench development in HTSC devices," *Cryogenics*, vol. 40, pp. 19–27, Nov. 1999.

[3] M. Fu, Z. Pan, Z. Jiao, H. Kumakara, K. Togano, L. Ding, F. Wang, Y. Zhang, Z. Chen, and J. Chen, "Quench characteristics and normal zone propagation of an $\mathrm{MgB_2}$ superconducting coil," *Superconducting Science and Technology*, vol. 17, pp. 16–163, Dec. 2003.

[4] A. Godeke, B. ten Haken, and H. H. J. ten Kate, "Scaling of the critical current in ITER type niobium-tin superconductors in relation to the applied field, temperature and uni-axial applied strain," *IEEE Trans. on Applied Superconductivity*, pt. 1, vol. 9, no. 2, pp. 161–164, 1999.

[5] M. Dhallé, P. Toulemonde, C. Beneduce, N. Musolino, M. Decroux, and R. Flükiger, "Transport and inductive critical current densities in superconducting $\mathrm{MgB_2}$," *Physica C*, vol. 363, p. 155, 2001.

[6] Y. Wang, T. Plackowski, and A. Junod, "Specific heat in the superconducting and normal state (2–300 K, 0–16 T), and magnetic susceptibility of the 38 K superconductor $\mathrm{MgB_2}$: evidence for a multicomponent gap," *Physica C*, vol. 355, p. 179, 2001.

[7] M. Schneider, D. Lipp, A. Gladun, P. Zahn, A. Handstein, G. Fuchs, S. L. Drechsler, M. Richter, K. H. Müller, and H. Rosner, "Heat and charge transport properties of $\mathrm{MgB_2}$," *Physica C*, vol. 363, p. 6, 2001.

[8] A. den Ouden, W. A. J. Wessel, H. J. G. Krooshoop, H. Van Weeren, H. H. J. ten Kate, G. A. Kirby, R. Ostojic, T. Taylor, and N. Siegel, "Design considerations for a 1 meter 10 T $\mathrm{Nb_3Sn}$ dipole magnet," *IEEE Trans. on Applied Superconductivity*, vol. 13, p. 1288.

[9] A. den Ouden, H. Van Weeren, W. A. J. Wessel, H. H. J. ten Kate, G. A. Kirby, N. Siegel, and T. Taylor, "Normal zone propagation in high-current density $\mathrm{Nb_3Sn}$ conductors for accelerator magnets," *IEEE Trans. on Applied Superconductivity*, vol. 14, p. 279, 2004.

[10] W. Goldacker, S. I. Schlachter, B. Liu, B. Obst, and E. Klimenko, "Considerations on critical currents and stability of $\mathrm{MgB^2}$ wires made by different preparation routes," *Physica C*, vol. 401, pp. 80–86, Jan. 2004.